



## Nonlinear Fe Model for Shear Strengthening of Simply Supported RC Beams with FRP DE Bars

Baisali Dutta <sup>1</sup>, Amar Nath Nayak <sup>1</sup>, Bharawaj Nanda <sup>1</sup>, Samir Dirar <sup>2</sup>

<sup>1</sup> Department of Civil Engineering, Veer Surendra Sai University of Technology, Burla – 768018, Sambalpur, Odisha, India

<sup>2</sup> Department of Civil Engineering, University of Birmingham, Birmingham, UK

Paper ID - 270120

### Abstract

Deep embedment (DE) is emerging as a potential and effective shear strengthening approach for existing reinforced concrete (RC) structures. A two-dimensional nonlinear finite element (NLFE) model for simply supported RC T-beams strengthened in shear with embedded carbon fibre reinforced polymer (CFRP) and steel bars is presented in this study. VecTor2, version 4.2, was used to create a two-dimensional NLFE model. To validate the nonlinear FE models, three sets of six simply supported RC T-beams from Breveglieri et al. (2015) are employed. Each set consists of two beams with vertical and inclined (45°) DE bars. Set one strengthens the beams with steel DE bars without vertical steel stirrups in the shear span. In the shear span, the beams of Sets two and three are reinforced with CFRP DE bars with vertical steel stirrups @180 mm c/c and @300 mm c/c, respectively. The above-mentioned NLFE model is validated by comparing experimental and predicted results for failure load, deflection, and failure mode. For both experimental and simulated beams, the fracture pattern is diagonal, and the failure mode is shear failure. The overall mean predicted/experimental loads at failure and deflection at failure ratios are 1.09 and 1.00, respectively, with corresponding standard deviations of 0.03 and 0.04. Following the validation of the proposed NLFE model's correctness, numerical parametric tests are conducted to determine the influence of concrete compressive strength and effective depth of RC T-beams on shear capacity of simply supported RC T-beams. The parametric analysis findings reveal that enhancing the cylinder compressive strength increases the predicted failure load while increasing the effective beam depth decreases it.

**Keywords:** Fibre reinforced polymer (FRP) bars, deep embedded (DE) technique, nonlinear finite element model, reinforced concrete (RC) T-beam, shear strengthening.

### 1. Introduction

Over the last two decades, there has been a significant increase in the need for shear strengthening and retrofitting of existing RC parts. Many times, fibre reinforced polymer (FRP) has been employed as a retrofitting element due to its potential qualities such as high strength to weight ratio, chemical and corrosion resistance, and ease of fabrication and handling. Many valuable research investigations on shear and flexure strengthening of RC beams with FRP composites have been undertaken and published [1,2].

Various shear strengthening methods, such as externally bonded (EB) [3-5] and near surface mounted (NSM) [6,7] FRP sheets or laminates, have been effectively used in the past to boost the shear capacity of existing RC structures. The main downside of these approaches is that FRP sheets or laminates debond from the concrete contact. To circumvent this sort of problem, the researchers devised another way of shear strengthening known as deep embedment (DE) [8,9]. The deep embedment (DE) approach is also known as the embedded through-section (ETS) technique [10,11]. For existing RC structures, this is a more

dependable and effective shear strengthening approach. Vertical holes are bored through the soffit of the RC beams or girders in the DE/ETS process, and high viscosity epoxy resin is then injected into the drilled holes, and FRP or steel bars are implanted into position.

Past research works have given an idea on DE shears strengthened RC beams. Valerio et al. [8] observed that the spacing between embedding bars should be near enough to prevent the formation of a shear discontinuity between the bars. Valerio et al. [9] have researched the deep embedment of FRP for concrete shear strengthening and discovered that the strengthening strategy is possible and effective for both RC and PSC beams of any size, even in the presence of existing steel stirrups. Shear failure occurs only when the bars are de-bonded from the concrete towards the top or bottom of the beams since DE/ETS strengthening is internal. Breveglieri et al. [11] discovered that vertical ETS bars give an improvement in load bearing capacity ranging from 5% to 68%. The slanted ETS bars have ensured a stronger strengthening effectiveness, as the load bearing capacity has increased from 53% to 136%.

\*Corresponding author. Tel: +919438275272; E-mail address: [baisali.dutta8@gmail.com](mailto:baisali.dutta8@gmail.com)

Despite a large number of experimental studies on shear strengthening of RC T-beams using the DE/ETS approach, only a few numerical studies have been undertaken. As finite element modelling (linear and nonlinear modelling) of RC T-beams has the ability to provide better knowledge about different parameters that influence the shear capacity of RC T-beams with a minimum cost involvement [12-14], it has the potential to provide better knowledge about different parameters that influence the shear capacity of RC T-beams with a minimum cost involvement. A nonlinear finite element (NLFE) model for DE-strengthened simply supported RC T-beams is presented in this study. This numerical model was then validated using experimental findings from the literature, such as the load-deflection curve and failure mechanisms. Finally, this validated model is utilised to investigate the effect of shear capacity on compressive strength and effective beam depth in simply supported RC T-beams.

## 2. Finite Element Model

A two-dimensional nonlinear finite element (NLFE) analysis is developed using VecTor2, version 4.2 [15]. A good number of basic models and element types from published literatures are used for developing a NLFE models. Based on accuracy and achieved results, the most accurate ones are adopted for NLFE models. The models used in NLFE modelling are briefly described in the following sections.

### 2.1 Geometric Modelling

Two-dimensional, four-node, plane stress rectangular elements are used to model the concrete, loading plate and support plate. The element has a uniform thickness and each node has two translational degrees of freedom. The rectangle may adopt any width and height but its accuracy decreases as the shape depart from a square. In that case, the rectangle with aspect ratio exceeding 3:2 has been avoided. Based on a mesh sensitivity analysis, which is not reported here for brevity, a maximum mesh size of 15 mm is used for the concrete, which gives converged results. The steel reinforcement, comprising of longitudinal reinforcement and shear links and DE bars are modelled using two-node truss elements.

### 2.2 Bond Property

Bond action plays a vital role in NLFE model. As the reinforcement adjacent to the concrete interface, resisting bond stresses act tangentially to the reinforcement. The type of bond modeling used in NLFE model, determines the stress-slip relationship for two separate cases i.e. confined bars and unconfined bars for DE bars.

### 2.3 Material Modelling

A smeared; rotating crack model is used for the concrete. In this model, the crack direction follows the principle stress direction. Therefore, the crack plane is considered as principal plane having zero shear stresses. Hence, after cracking, the modeling of concrete shear behavior is not required. Based on the research work of Capo et al. [12, 13], the Poisson's ratio is considered as 0.15

Eq. 1, originally proposed by Thorenfeldt et al. [16], is used to model the pre-peak behavior of concrete in compression.

$$f_{ci} = -\left(\frac{\varepsilon_{ci}}{\varepsilon_p}\right) f_p \frac{n}{n-1+(\varepsilon_{ci}/\varepsilon_p)^k} \text{ for } \varepsilon_{ci} < 0 \quad (1)$$

Where  $f_{ci}$  is the principal compressive stress,  $\varepsilon_{ci}$  is the principal compressive strain,  $f_p$  is the peak compressive stress,  $\varepsilon_p$  is the strain corresponding to  $f_p$ , which is a parameter equal to  $(0.80+f_p/17)$ ,  $k$  is equal to 1.0,  $n$  is the curve fitting parameter, which is the difference between the initial tangent stiffness  $E_c$ , and secant stiffness,  $E_{sec}$ .

The post-peak behavior of concrete in compression is modelled using the following equations reported in the literature [15],

$$f_{ci} = (1 - c)f_{ci}^a + cf_{ci}^b \quad (2)$$

$$c = 4 \left( \frac{f_p - f_c'}{f_c'} \right), \quad 0 \leq c \leq 1 \quad (3)$$

$$f_{ci}^a = -f_p \left( \frac{\varepsilon_{ci}}{\varepsilon_p} \right) e^{\left\{ 1 - \left( \frac{\varepsilon_{ci}}{\varepsilon_p} \right) \right\}} \quad (4)$$

$$f_{ci}^b = -\left(\frac{\varepsilon_{ci}}{\varepsilon_p}\right) f_p \frac{n}{n-1+(\varepsilon_{ci}/\varepsilon_p)^k} < -0.2f_p \quad (5)$$

$$n = \left( \frac{E_c}{E_c - E_{sec}} \right) = \left( \frac{5000 \sqrt{f_c'}}{5000 \sqrt{f_c'} \frac{f_p}{\varepsilon_p}} \right) \quad (6)$$

Where,  $f_c'$  in the above equations denotes the unconfined uniaxial concrete cylinder strength. The post-peak response is assumed to have a residual value of  $0.2f_p$  when the concrete is sufficiently confined. Compression softening is modelled using the following equations as suggested in the literature [15], considering  $\varepsilon_{c1}$  as the principal tensile strain. Fig. 1 shows the pre-peak and post-peak concrete compression response.

$$f_p = \frac{f_c'}{1+0.55C_d} \quad (7)$$

$$C_d = 0.27 \left( \frac{-\varepsilon_{c1}}{\varepsilon_p} - 0.37 \right), \quad 0 \leq C_d \leq 50 \quad (8)$$

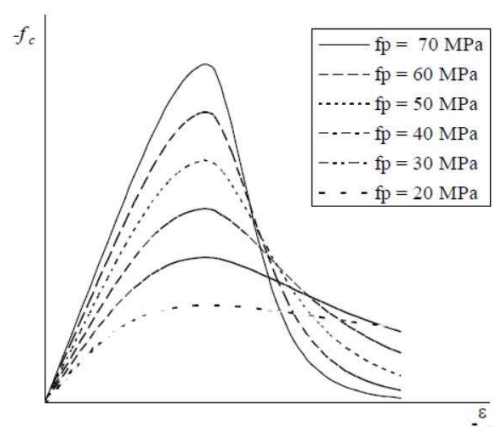


Fig.1. Pre-peak and post-peak concrete compression response [15].

A linear relationship up to concrete cracking was used for modeling the tensile behavior of concrete. For post-cracking, the following bilinear tension softening model is used.

$$\varepsilon_{ch3} = 0.64\varepsilon_{ch} + \varepsilon_{cr} \quad (9)$$

$$\varepsilon_{ch4} = 6.8\varepsilon_{ch} + \varepsilon_{cr} \quad (10)$$

$$\varepsilon_{ch} = \frac{G_f}{L_{ref} f_{cr}} \quad (11)$$

where  $\varepsilon_{cr}$  is the cracking strain,  $\varepsilon_{ch3}$  is the tensile strain corresponding to  $0.2f_{cr}$ ,  $\varepsilon_{ch4}$  is the strain at which the tension softening stress diminishes to zero,  $\varepsilon_{ch}$  is the characteristic strain of the tension softening curve,  $G_f$  is the concrete fracture energy, which is automatically calculated by VecTor2 [15] and  $L_{ref}$ , taken as half the crack spacing, is the distance over which the crack is assumed to be uniformly distributed.

The stress-strain model for the steel reinforcement as well as the loading and support plates had an initial linear-elastic response followed by a yield plateau and a nonlinear strain-hardening phase until rupture. Bond failure was not the governing failure mode in the modelled beams, particularly for the DE/ETS steel bars. This approach was successfully used by Qapo et al. [13] to model shear-strengthened concrete girders.

### 3. Model Validation

According to the literature, the RC T-beams of Breveglieri et al. [11] are used for model validation. Three sets of simply supported RC T-beams (Fig. 2) from the literature are evaluated for validation of the proposed numerical model. Each set consists of two beams with vertical and inclined (45°) DE bars. Set one strengthens the beams with steel DE bars without vertical steel stirrups in the shear spans 0S-S180-90 and 0S-S180-45. In the shear spans marked as 2S-C180-90, 2S-C180-45, 4S-C180-90, and 4S-C180-45, the beams of Sets two and three are strengthened with CFRP DE bars with vertical steel stirrups @180 mm c/c and 300 mm c/c, respectively.

The concrete average compressive strength (fcm) of the beams was determined at 28 days by performing direct compression tests on cylinder specimens of 150 mm diameter and 300 mm height in accordance with EN 206-1 (2004) [17]. It is 24.7 and 29.7 MPa at 28 days and the day of the test (about 255 days) for the first batch (0S-Series and 2S-Series), respectively, and 27.6 and 32.3 MPa at 28 days and the day of the test (approximately 250 days) for the second batch (4S-Series and CFRP ETS strengthened beams). High bond steel bars with diameters of 6, 10, 8, 12, and 24 mm are utilised for internal beam reinforcement. According to the Italian Construction Code [18], the steel class is B 450 C (fyk = 450 MPa). The yield stress and tensile strength were determined using uniaxial tensile tests done in accordance with the requirements of UNI EN ISO

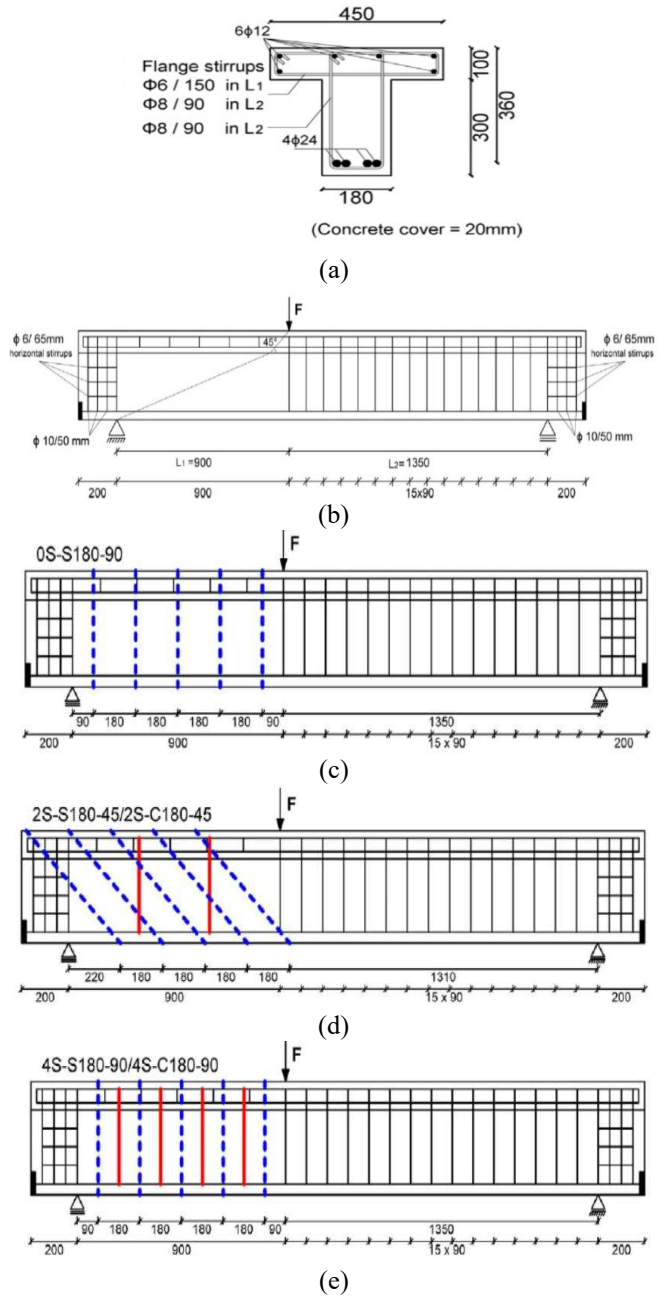


Fig.2. Detail of Strengthened beams (All dimensions in mm) [11] (a) Cross-section (b) Un-strengthened beam 0S(c) 0S-S180-90 (d) 2S-C180-45, (e) 4S-C180-90

6892-1:2009 [19]. For the steel bars of 6, 8, 10, 12 and 24 mm diameter it is obtained an average yield stress of 574 MPa ( $\varepsilon_{sy} = 0.287\%$ ), 505 MPa ( $\varepsilon_{sy} = 0.253\%$ ), 549 MPa ( $\varepsilon_{sy} = 0.275\%$ ), 527 MPa ( $\varepsilon_{sy} = 0.264\%$ ) and 598 MPa ( $\varepsilon_{sy} = 0.299\%$ ), and an average tensile strength of 667 MPa, 594 MPa, 642 MPa, 617 MPa and 708 MPa, respectively.

The ETS steel bars used in the beams are of the same class as the bars used for flexural reinforcement and steel stirrups. Sikadur 32 N epoxy-based glue was utilised to bind the ETS steel bars to the concrete substrate. The tensile behaviour of this glue was studied using direct tensile testing according to ISO 527-2 [20]. The average tensile strength and elasticity modulus were calculated to be 20.7 MPa and 3.27 GPa. The Master Brace BAR 8 CFS [21]

carbon fibre sandblasted 8 mm rod has an elasticity modulus of 160 GPa and an ultimate strain of 1.2 percent.

The beams are tested under three-point stress to ensure that they can fail under shear. The beam is constructed in such a way that the failure is limited to a single spot ( $L_1$ ) inside the beam. This beam's shear span ( $L_1$ ) is calculated as 2.5 times its effective depth (d) (i.e.  $L_1/d = 2.5$ ). In the shear span, 8 mm diameter shear links separated at 90 mm c/c are supplied to prevent shear failure within  $L_2$  ( $L_2$ ).

By comparing experimental and predicted load-deflection findings, failure mechanism, and crack patterns, the FE model was validated. The observed and predicted load-deflection curves are quasi-linear up to crack development, as seen in Fig. 3. The FE model adequately predicts the pre-cracking stiffness, indicating that the boundary conditions and elastic constants are well described. After crack development, the load-deflection curves of the experimental

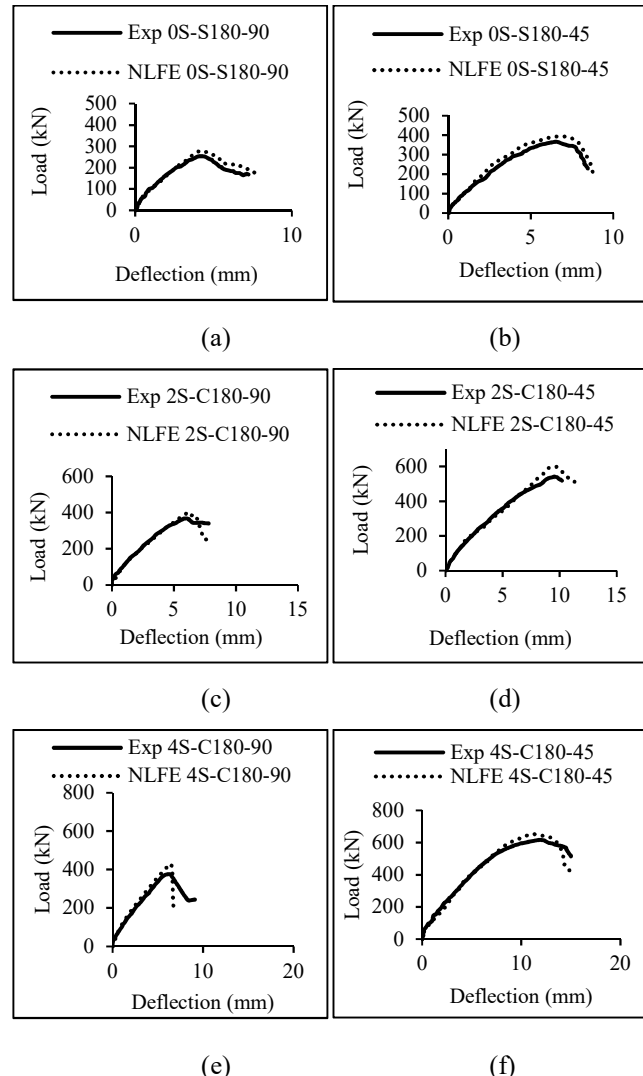


Fig.3. Experimental [11] and NLFE-predicted Ultimate load-deflection curves: (a) 0S-S180-90, (b) 0S-S180-45, (c) 2S-C180-90, (d) 2S-C180-45, (e) 4S-C180-90, (f) 4S-C180-45

and numerical models become nonlinear due to stiffness loss. The post-cracking stiffness is also adequately simulated in the NLFE model. The post-cracking rigidity continues to deteriorate as the load is gradually increased until the model collapses. The load-deflection curve during failure shows a quick decline in load at peak load, indicating a brittle failure.

Images showing crack patterns of experimental failure modes of strengthened and un-strengthened RC T-beams, as well as the failure modes of the NLFE model, are shown in Fig. 4. It is said that all of the crack patterns are diagonal in form, with shear failure mechanisms. All of the predicted crack patterns of NLFE models are almost identical to the experimental crack patterns. The mean predicted/experimental load bearing capacity ratio and its standard deviation are determined to be 1.09 and 0.03,

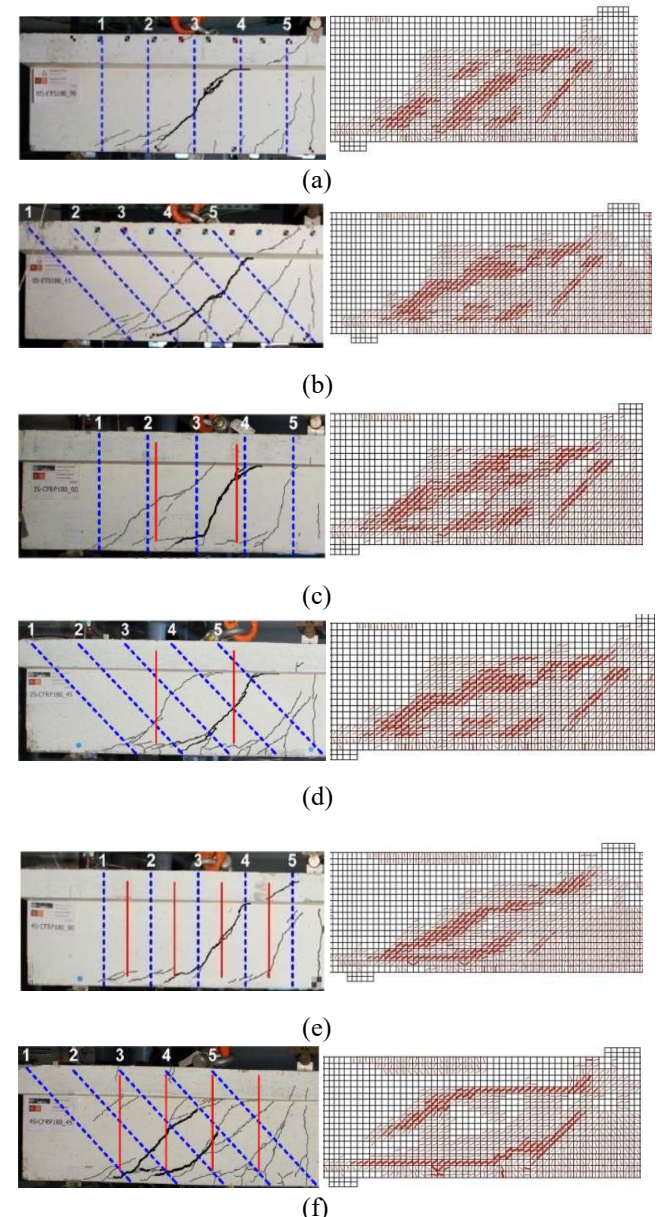


Fig.4. NLFE predicated and experimental failure mode in simply supported RC T-beam [11]: (a) 0S-S180-90, (b) 0S-S180-45, (c) 2S-C180-90, (d) 2S-C180-45, (e) 4S-C180-90, (f) 4S-C180-45

respectively. Similarly, the mean predicted/experimental ratio and standard deviation of the deflection at peak load are 1.00 and 0.04, respectively. As a result, the beams are accurately modelled.

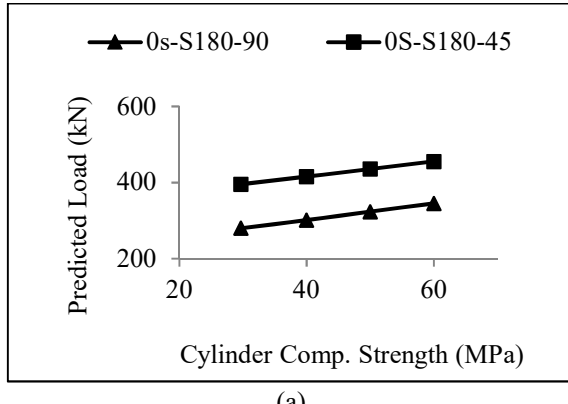
#### 4. Parametric study

Following the validation of the NLFE models, numerical parametric research was conducted to explore the influence of concrete compressive strength and effective depth on shear capacity of simply supported RC T-beams.

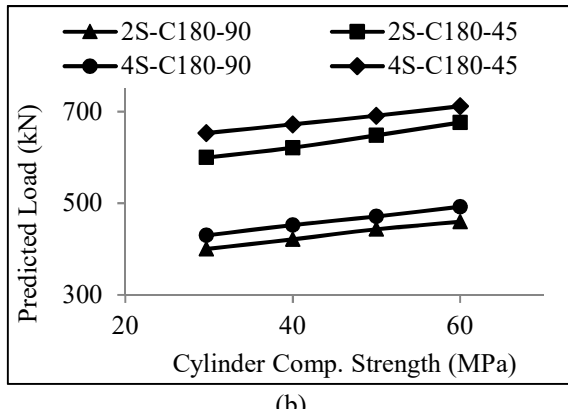
##### 4.1 Concrete cube compressive strength

The compressive strength of concrete has a significant impact on the shear capacity of RC structures. The influence of concrete compressive strength on the simulated RC T-beams follows a similar pattern to that seen in the study of Breveglieri et al [11]. Six beams are assumed similar for the parametric study: 0S-S180-90, 0S-S180-45, 2S-C180-90, 2S-C180-45, 4S-C180-90, 4S-C180-45. Cylinder compressive strength values of 30, 40, 50, and 60 MPa are investigated for each simply supported RC T-beam. The influence of cylinder compressive strength on anticipated force at failure for all six types of RC T-beams is shown in Fig. 5.

For simply supported RC T-beams, raising the cylinder compressive strength from 30 MPa to 60 MPa raised the projected failure load by 32-39 percent. From the

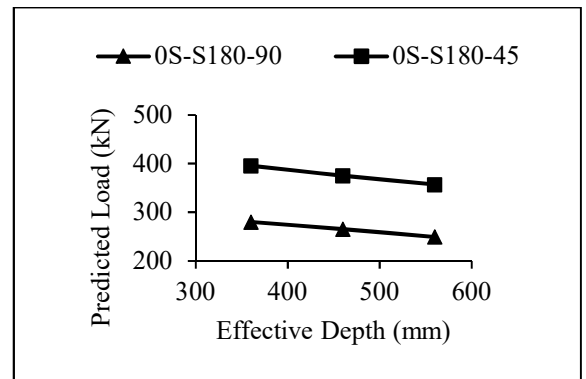


(a)

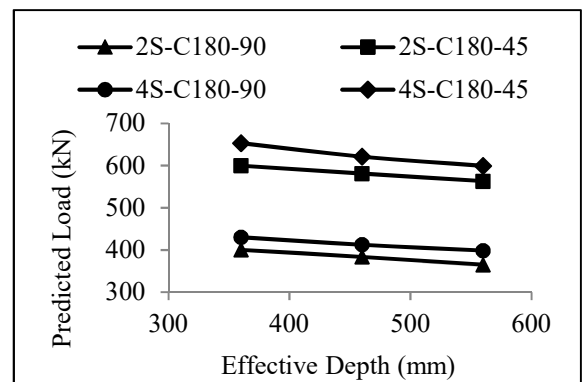


(b)

Fig. 5. Effect of cylinder compressive strength on the predicted failure load of strengthened RC T-beams: (a) 0S Series (b) 2S and 4S series.



(a)



(b)

Fig. 6. Influence of effective beam depth on the predicted failure load of strengthened RC T-beams: (a) 0S Series (b) 2S and 4S series.

study it is clear that the inclined DE bars has more shear capacity than that of vertically installed DE bars.

##### 4.2 Effective beam depth (d)

In this research, NLFE models with effective beam depths of 360 mm, 460 mm, and 560 mm for each beam type of 0S-S180-90, 0S-S180-45, 2S-C180-90, 2S-C180-45, 4S-C180-90, and 4S-C180-45 are evaluated to determine the effect of effective depth on load bearing capability. The flange dimension changes with beam depth, while other parameters such as longitudinal reinforcement diameter, stirrups and DE bars, mesh density, and steel reinforcement ratio remain constant. Figure 6 depicts the effect of effective beam depth on predicted failure load. According to the figure, extending the beam depth from 360 mm to 560 mm reduces the expected failure stress of a simply supported RC T-beam by 7% - 9%. The reduction in predicted failure load with increase in depth may be due to fact that moment of resistance of any beam increases with its effective depth.

#### 5. Conclusions

From existing literature, an NLFE model for simply supported RC T-beams reinforced in shear with DE steel and CFRP bars was created and verified. According to the observations, the mean ratios of predicted / experimental loads and deflection at failure are 1.09 and 1.0, respectively,

with corresponding standard deviations of 0.03 and 0.04. The parametric analysis was conducted to explore the effect of concrete cylinder compressive strength and effective beam depth on anticipated failure load. The failure load and shear force capacity of the RC T-beams were enhanced by employing 45 inclined DE CFRP and steel bars. This is due to the inclined position of the DE bars being perpendicular to the RC T-beams' diagonal cracking pattern. Furthermore, raising the concrete cylinder compressive strength increases the anticipated shear strength capacity and failure load. The increase in effective beam depth, on the other hand, decreases the failure load.

### Acknowledgements

The UK India Education and Research Initiative (UKIERI) has provided financial support under Grant UKIERIUGC 2017-18/17.

### Disclosures

Free Access to this article is sponsored by SARL ALPHA CRISTO INDUSTRIAL.

### References

1. Pellegrino C, Modena C. Fiber-reinforced polymer shear strengthening of reinforced concrete beams: Experimental study and analytical modeling. *ACI Structural Journal*, 2006; 103(5):720.
2. Mofidi A, Thivierge S, Chaallal O, and Shao Y. Behavior of reinforced concrete beams strengthened in shear using L-shaped CFRP plates: Experimental investigation. *Journal of composites for construction*, 2014; 18(2): 04013033.
3. Bousselham A, Chaalal O. Shear strengthening reinforced concrete beams with fibre-reinforced polymer: assessment of influencing parameters and required research. *ACI Structural Journal*, 2004; 101(2):219–227.
4. Dirar S, Lees JM, Morley C. Phased Nonlinear Finite-Element Analysis of Pre-cracked RC T-Beams Repaired in Shear with CFRP Sheets. *ASCE Journal of Composites for Construction*, 2013;17(4):476-487.
5. Kumari A, Patel SS, Nayak AN. Shear Strengthening of RC Deep Beam Using Externally Bonded GFRP Fabrics. *Journal of Institute of Engineering India Series A*, Springer, 2018:341-350.
6. Chaallal O, Mofidi A, Benmokrane B, and Neale K. Embedded through-section FRP rod method for shear strengthening of RC beams: Performance and comparison with existing techniques, *ASCE Journal of Composites for Construction*, 2011;15(3): 374-383.
7. Mofidi A, Chaallal O, Cheng L, and Shao Y. Investigation of near-surface-mounted method for shear rehabilitation of reinforced concrete beams using fiber reinforced-polymer composites, *ASCE Journal of Composites for Construction*, 2016; 20(2):1-14.
8. Valerio P, Ibell TJ, Shear strengthening of existing concrete bridges. *Proceedings of the Institution of Civil Engineers - Structures and Buildings*, 2003;156(1):75–84.
9. Valerio P, Ibell TJ, and Darby AP., Deep embedment of FRP for concrete shear strengthening, *Proceedings of the Institution of Civil Engineers Structures and building*, 2009; 162(5): 311–21.
10. Mofidi A, Chaallal O, Benmokrane B, and Neale KW. Experimental tests and design model for RC beams strengthened in shear using the embedded through section FRP method, *ASCE Journal of composites for construction*, 2012;16(5): 540–550.
11. Breveglieri M, Aprile A, and Barros JAO. Embedded Through-Section shear strengthening technique using steel and CFRP bars in RC beams of different percentage of existing stirrups, *Composite Structures*, 2015;126: 101-113.
12. Qapo M., Dirar S., Yang J., Elshafie M.Z.E.B., Nonlinear finite element modelling and parametric study of CFRP shear-strengthened prestressed concrete girders. *Construction and Building Materials*, 76, 245-255, 2015.
13. Qapo, M., Dirar, S. and Jemaa, Y., Finite element parametric study of reinforced concrete beams shear-strengthened with embedded FRP bars. *Composite Structures*, 149, 93-105, 2016.
14. Dutta B., Sogut, K., Dirar S., Nayak A. N., Nanda B., Theofanous, M. and Faramarzi,A. (2019). "Nonlinear Finite Element Analysis of Reinforced Concrete Beams Strengthened in Shear with Embedded Steel Bars." *Proceedings of the 9th Biennial Conference on Advanced Composites in Construction 2019* held at the University of Birmingham, UK pp, 239-244, 3rd - 5th September 2019.
15. Wong PS, Vecchio FJ, and Trommels H, *VecTor2 & FormWorks User's Manual (Second Edition)*, University of Toronto, Canada, 2013.
16. Thorenfeldt E, Tomaszewicz A, and Jensen JJ. Mechanical properties of high strength concrete and applications in design, In *Proceedings of the symposium on the utilization of high-strength concrete*, Stavanger, 15<sup>th</sup>–18<sup>th</sup>June 1987.149–159.
17. European Committee for Standardization. EN 206–1 Concrete – Part 1: Specification, performance, production and conformity. 2004.
18. Italian Construction Code. C.S.L.P. *NuoveNormeTecniche per le Costruzioni* DM 14 gennaio 2008 - GazzettaUfficiale n. 29 del 4 febbraio 2008. 2009.
19. European Committee for Standardization. UNI EN ISO 6892–1:2009 Metallic materials - Tensile testing - Part 1: Method of test at room temperature. 2009.
20. European Committee for Standardization. ISO 527–2:2012. Plastics - Determination of tensile properties - Part 2: Test conditions for moulding and extrusion plastics. 2012.
21. BASF Construction Chemicals Italia Spa. Technical sheet MasterBrace BAR 8 CFS. <http://www.master-builders-solutions.bASF.it/>.